# Electromagnetic Noise from an Ion Engine System

I. Kudo,* K. Machida,* Y. Toda,† and H. Murakami†
*Electrotechnical Laboratory, Ibaraki, Japan*

**The conducted and radiated emission of electromagnetic noise from an ion engine system was measured. The measured data were compared with MIL-STD-461A and a specification for the ion engine system on ETS-III, and found to satisfy the latter specification. During the conducted emission measurements, three discharge modes were observed and their oscillating characteristics were compared. An ion acoustic wave was generated spontaneously during a low discharge voltage mode. A relatively narrow discharge voltage range was found to minimize the noise.**

## Introduction

AN ion engine system of 5-cm diameter is being developed for use as a satellite attitude control thruster system. The small diameter ion engine is one of four experiments on the Japanese engineering test satellite (ETS)-III, which will be launched in 1982 to a 1000-km altitude, circular orbit by an N-7 vehicle. Since the ion thruster itself is a device that generates an electromagnetically noisy plasma and its power conditioner consists of dc-dc converters and dc-ac inverters that use high-frequency transistor switching, high-level noise emissions are to be expected from both components. Although noise specification for equipment onboard the ETS-III satellite complied with MIL-STD-461A Notice-3, this was relaxed for the ion engine system because of its inherent noise characteristics. For the ion engine system, no broadband requirement is given for conducted emission (CE), and 100 $dB_{\mu V}$ is permitted in the frequency range from 14 kHz to 1 MHz for narrow-band radiated emission (RE). For broadband RE, 40 dB above the specification of MIL-STD-461A is permitted.

This paper describes the measurement of electromagnetic noise emitted from the ion engine system and an investigation into discharge plasma modes when the discharge voltage is varied.

## Ion Engine System and Test Facilities

The ion engine system consists of a thruster, a power supply unit, and a command interface. The latter two items are components of the power conditioner. The command interface receives signals from a command generator and operates the power supply unit sequentially. It also controls a discharge voltage-main vaporizer loop and a keeper voltage-neutralizer vaporizer loop. Telemetry signals and the status of the engine are monitored on the command generator panel. The specification for the power supply unit is shown in Table 1.[1,2]

The thruster was placed on a flange of a glass cylinder attached to an ion engine test chamber. The glass cylinder was 60-cm in diameter, 1-m long, and was connected to the test chamber by a gate valve. Adoption of the glass cylinder made possible the measurement of noise emitted from the discharge chamber and plasma beam. The power conditioner was set up on a $2 \times 2$-m copper ground plane.

Presented as Paper 81-0724 at the AIAA/JSASS/DGLR 15th International Electric Propulsion Conference, Las Vegas, Nev., April 21-23, 1981; submitted April 29, 1981; revision received May 21, 1982.


*Senior Research Staff, Advanced Engineering Division, Member AIAA.
†Research Staff, Advanced Engineering Division.

A typical operational sequence for the ion thruster is shown in Fig. 1. The number in this figure indicates the beginning of engine operation. The following is a description of the different operating states.

1) SW on: the logic circuits are activated. This state is initiated by sending an enable command from the command generator.

2) Start: the vaporizer power supplies (PS6 and 9), cathode heater power supplies (PS4 and 8), and the isolator power supply (PS10) are turned on.

3) N on: the neutralizer is ignited. In this state, the neutralizer keeper voltage drops from 300 to 24 V, while the keeper current increases from 0 to 0.25 A.

4) M on: the main cathode is ignited. In this state, the cathode keeper voltage drops from 300 to 15 V, while the current increases from 0 to 0.3 A.

5) D on: in this state, a plasma is generated in the discharge chamber. The discharge voltage drops from an initial high level to 40 V, while the discharge current may be varied from 0 to 0.4 A.

6) HV on: in this state, an ion beam is ejected and the ion engine generates thrust.

Operating states 2-5 are automatically sequenced by sending a start command. State 6 is initiated by a continue command. A power profile corresponding to the enumerated states is also shown at the bottom of Fig. 1 as input power. Although noise measurements should be made for all of the states, this procedure is too time consuming. When the power profile in Fig. 1 is considered, the states of start and HV on consume the most power. Therefore, extensive measurements were done at these two states. This test abbreviation is in agreement with Ref. 3.

The test matrix used is shown in Fig. 2. In this figure, X indicates that the measurement has been made and D and T indicate whether a dummy thruster or an ion thruster was connected to the power conditioner, respectively. The dummy thruster consists of resistors and transistor switches. The resistance values in the dummy thruster simulate each part of the thruster. The dummy thruster was designed to minimize noise emission from the internal electronic circuits.

In Fig. 2, Int. C is a line between the command interface and the power supply unit. In order to investigate noise levels between the thruster and the power conditioner, noise on the anode, cathode keeper (CK), neutralizer keeper (NK), screen ($J_B$) and accelerator ($I_A$) lines were measured.

## Conducted Emission Measurements

A block diagram of a CE measurement is shown in Fig. 3. As mentioned previously, the measurements were performed with both the dummy and the thruster as a load on the power conditioner. The results of noise measurements of the power lines with the dummy and the thruster as loads are shown in

**Table I Specification for the power supply unit**

| Part | Level[a] | Voltage | Current | Type |
|---|---|---|---|---|
| Screen | NL | 1.0 kV | 30 mA | dc |
| Accel | NL | −1.0 kV | 1 mA | dc |
| Discharge | NL | 40 V | 0.35 A | dc |
| Cathode | NL | 5 V | 5 A | ac |
| Heater | IL | 1.6 V | 2.5 A | |
| Cathode | NL | 15 V | 0.3 A | dc |
| Keeper | SL | 300 V | 5 mA | |
| Cathode vaporizer | ML | 3.5 V | 2 A | ac |
| Neutralizer | NL | 5 V | 5 A | ac |
| Heater | IL | 1.6 V | 2.5 A | |
| Neutralizer | NL | 24 V | 0.25 A | dc |
| Keeper | SL | 300 V | 5 mA | |
| Neutralizer vaporizer | ML | 2.6 V | 1.5 A | ac |
| Isolator | NL | 3 V | 1 A | ac |
| | HL | 5 V | 1.6 A | |

[a] NL, nominal level; HL, high level; IL, idling level; ML, maximum level; SL, start level.

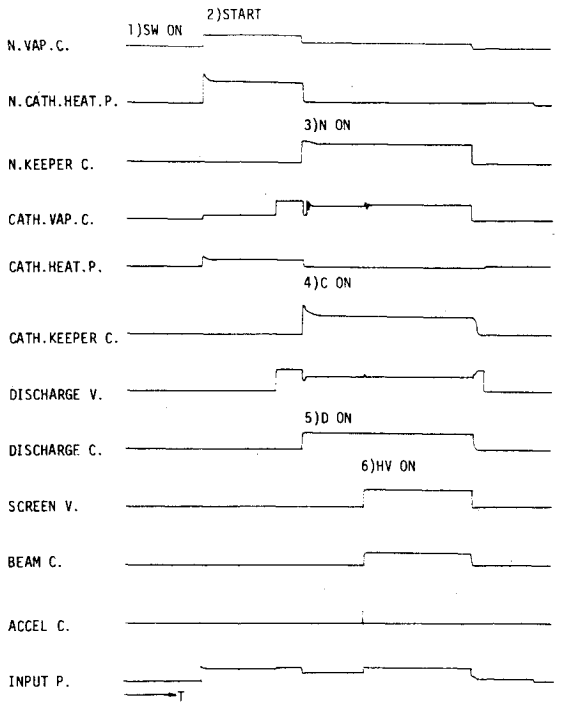


**Fig. 1 Typical operational sequence.**

| TEST ITEM | CE01,02,03,04 | | | | | | | | | | | | | | | | | | | | RE02 | | RE04 | |
|---|---|---|---|---|---|---|---|---|---|---|---|---|---|---|---|---|---|---|---|---|---|---|---|---|
| LINE I.D. | PWR | | CMD | | TLM | | INT.C. | | ANODE | | C.K. | | N.K. | | $J_B$ | | $I_A$ | | - | | - | | | |
| LOAD / STATUS | D | T | D | T | D | T | D | T | D | T | D | T | D | T | D | T | D | T | D | T | D | T | D | T |
| 1) SW ON | X | X | | X | | X | | | | | | | | | | | | | | | | | | |
| 2) START | X | X | X | X | X | X | X | X | X | X | X | X | X | X | | | | | | | | X | | X |
| 3) N ON | X | X | | X | | X | | | | | | | | X | | | | | | | | | | |
| 4) C ON | X | X | | X | | X | | | | | | X | | X | | | | | | | | | | |
| 5) D ON | X | X | | X | | X | | | | X | | | | | | | | | | | | | | |
| 6) HV ON | X | X | X | X | X | X | X | X | X | X | X | X | X | X | X | X | X | X | | | | X | | X |

**Fig. 2 A test matrix.**

Figs. 4a and 4b, respectively. No remarkable spectral differences were found between the dummy and the thruster measurements. This suggests that data taken with the dummy can be used for conducted electromagnetic interference (EMI) evaluation of the ion engine system. In fact, the electromagnetic compatibility with the ETS-III satellite was confirmed with the dummy ion thruster.

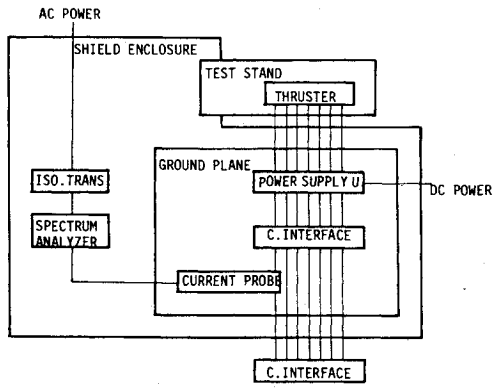


**Fig. 3 Schematic diagram of CE measurement.**

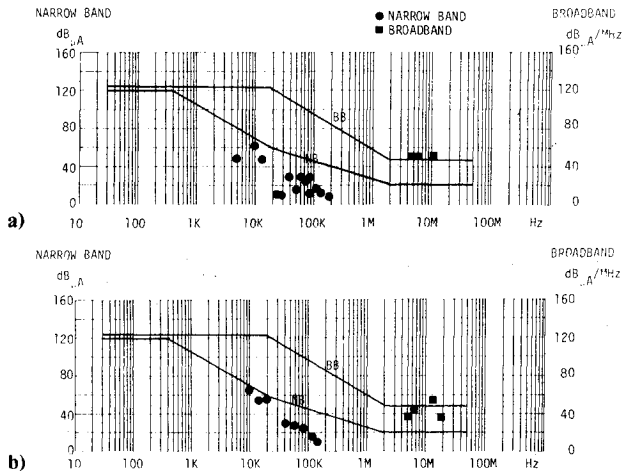


**Fig. 4 CE measurement result for power line a) dummy thruster and b) ion thruster.**

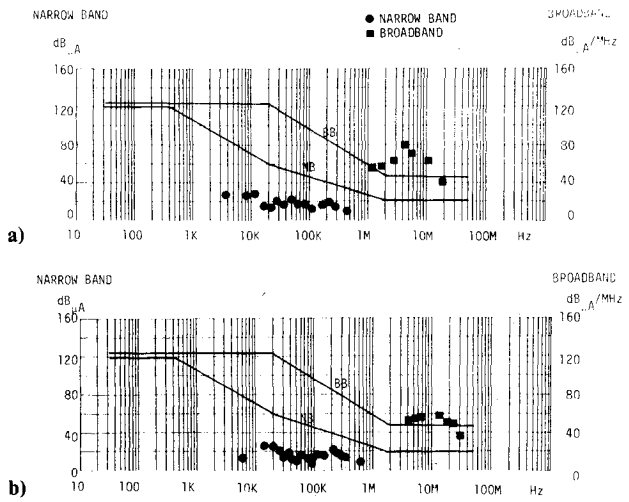


**Fig. 5 CE measurement result for a) command line (ion thruster) and b) telemetry line (ion thruster).**

Figures 5a and 5b show the test results for the command and telemetry lines with the real thruster in use. The command line noise was 20 dB above the MIL-STD-461A specification at frequencies of 5 and 12 MHz. Feedthrough capacitors were added for suppression of broadband noises in the appropriate command lines.

No difficulty was found in meeting the ETS-III ion engine system specifications. The noise data during the HV on state

were considered to be representative when compared to all power CE data.

## Radiated Emission Measurements

Electrostatic and electromagnetic interferences were measured when the ion thruster was connected to the power conditioner by following MIL-STD-462 methods. The equipment setup inside the shielded enclosure is shown in Fig. 6. The power conditioner was placed outside the glass cylinder because its heavy weight might have stressed the glass cylinder. In order to recognize easily whether the noise was from the power conditioner or from the thruster, two antennas were used. Noise from the thruster was measured by the antenna at A and the noise from the power conditioner was measured by the antenna at B. The test results of electrostatic radiation (RE)-02 at position A are shown in Fig. 7a and the results at position B are shown in Fig. 7b. No notable difference was observed for the antenna positions except that the broadband noise of B in the frequency range from 10 to 100 MHz was a little higher than that of A. No remarkable difference was apparent on the analyzer when vertical and horizontal polarizations of a biconical antenna were compared. As compared with the high broadband noise that appeared on the command lines in the frequency range up to 15 MHz, noise was observed at a higher frequency range for radiated emission measurements. Noise emissions radiated from the thruster seem to be the difference. For the former, filter insertion was used to reduce the noise. However, radiated noise from the thruster itself can not be reduced by a filter. The noise specification for the ion engine system on ETS-III was relaxed a great deal, in consideration of this situation. Plasma peculiar peaks (narrow-band) were not observed for either A or B antennas.

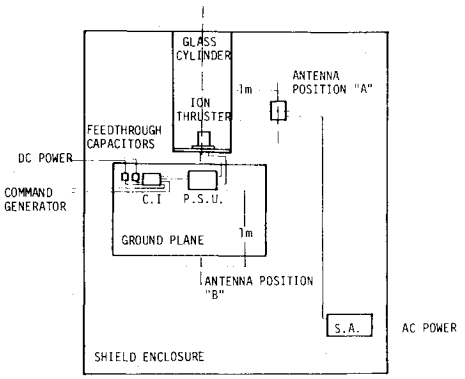


**Fig. 6 RE measurement set up in a shield enclosure.**

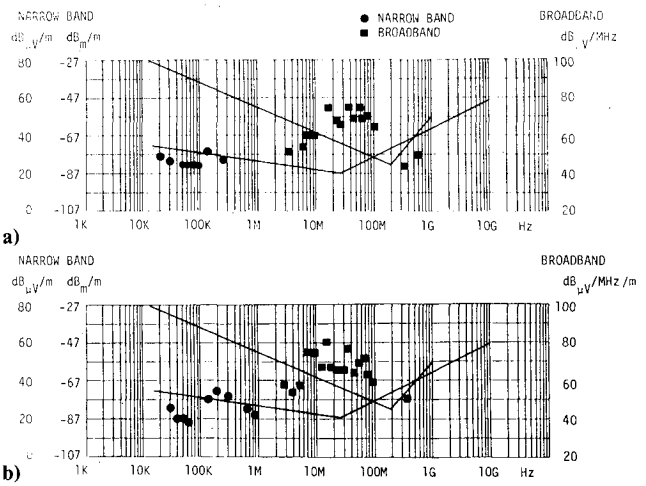


**Fig. 7 RE02 measurement result a) antenna position A and b) antenna position B.**

The results of electromagnetic interference (RE)-04 are shown in Fig. 8 for antenna position A. Though a slight out-of-specification condition was observed at 200 Hz, the 5-kHz fundamental frequency and its higher harmonics seemed to be controlled. The magnetic field noise parallel to the thruster axis was 10 dB higher than that perpendicular to the axis.

The electromagnetic compatibility between the ion engine system and the ETS-III satellite has been confirmed by using an EMI simulator. The details are described in Ref. 4.

## Thruster Discharge Mode

Some strange coherent peaks appeared on the spectrum analyzer during the CE measurements. The measurements were aimed at evaluating the interference of the thruster with the power conditioner. The peaks were found when the anode line was measured, and they sometimes disappeared. A parametric study was performed in order to ascertain the cause of the wave generation mechanism, with the thruster screen voltage and discharge current maintained constant. Figure 9 shows variations of cathode keeper current, beam current, accelerator current, and ion production cost for the discharge voltage. The increase in the discharge voltage resulted in an increase in beam current and a decrease in the accel current. That is, beam focusing was improved. There was a gradual decrease in cathode keeper current as the discharge voltage was increased. When the discharge voltage reference was set to 46 V, the discharge stopped due to the low propellant flow.

Three discharge modes were observed on the spectrum analyzer as shown in Fig. 10. When the discharge voltage was

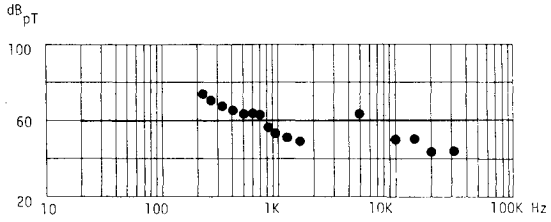


**Fig. 8 RE04 measurement result at antenna position A.**

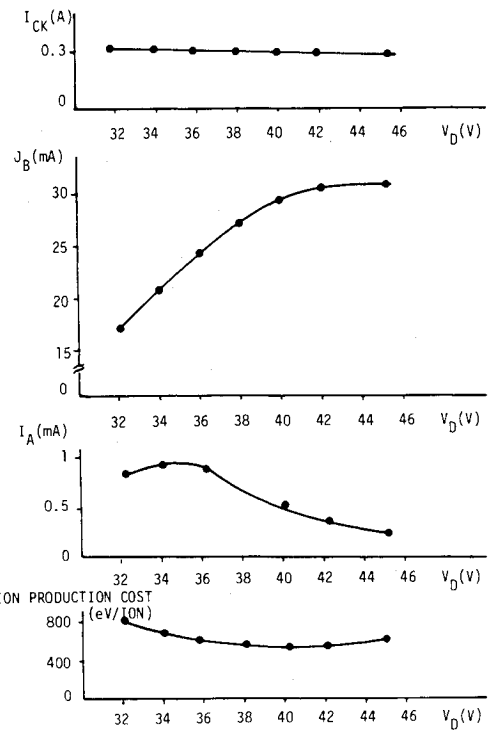


**Fig. 9 Major parameter changes against discharge voltage.**

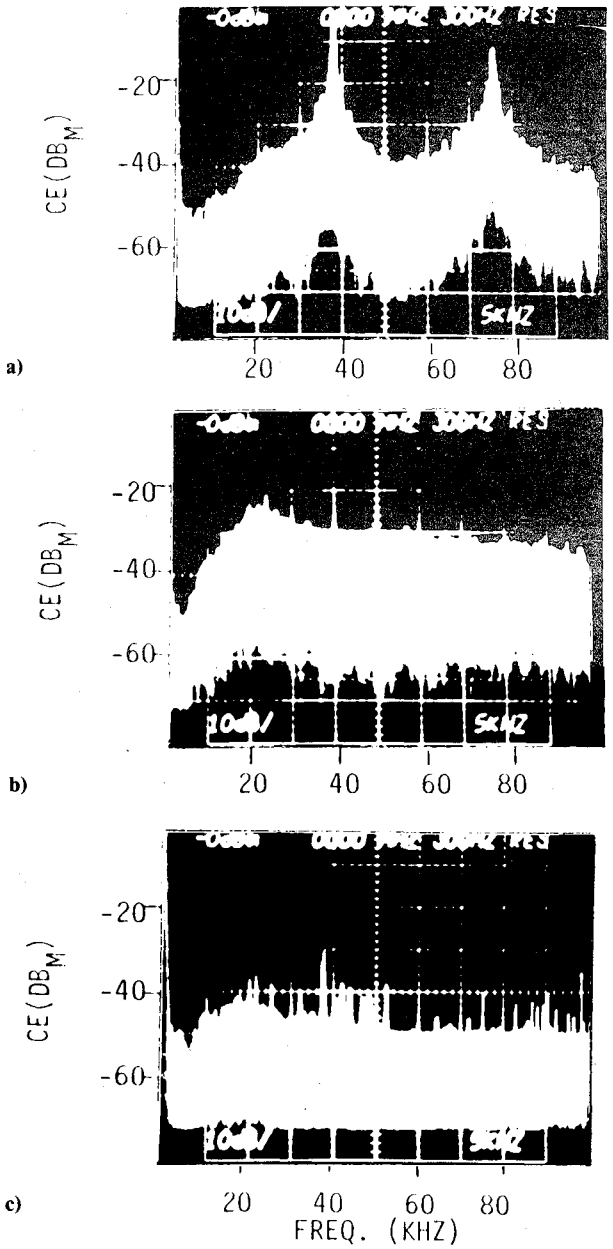


Fig. 10 Discharge voltage a) below 36 V, b) range of 36-38 V, and c) above 38 V.

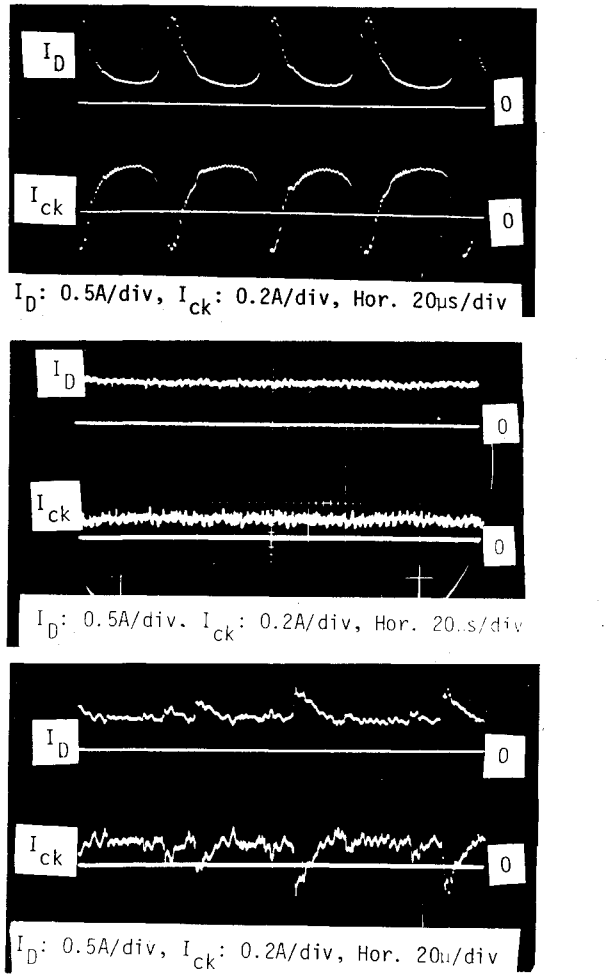


Fig. 11 Discharge voltage a) below 36 V, b) range of 36-38 V, and c) above 38 V.

changed, the first mode appeared under 36 V for both the anode and the cathode keeper lines and it was found that coherent waves were generated spontaneously. The wave amplitudes were 30 dB higher than the MIL specification (Fig. 10a). When the discharge voltage was increased to 36 V, the noise level dropped as much as 50 dB with reference to the already noted condition (Fig. 10b). This mode existed within a small discharge voltage range of 36-38 V. When the discharge voltage was increased further, the noise again increased. The high noise level supposedly is caused by plasma turbulence. This mode is shown in Fig. 10c. Time domain waveforms of discharge current and cathode keeper current are shown in Figs. 11a-c. It was found from the figure that these currents were complementary to each other.

As far as the coherent wave of Fig. 10a is concerned, it is considered to be an ion acoustic wave which is the result of the two-stream instability.[5-7] It occurs when the keeper discharge interacts with the main discharge plasma. This wave could not be observed on the cathode keeper line when only the cathode keeper discharge was on, nor could it be observed on a neutralizer keeper current line. The ion acoustic velocity is expressed as

$$V = nf_n L/2 \tag{1}$$

where $L$ is the distance between keeper electrode and anode and $n$ is the mode number. For $n=1$, the velocity is about $70 \times 10^4$ cm/s. When the number $n$ is increased, wave velocity is increased and wave amplitude is reduced. There is a cutoff beyond which no higher frequencies are observed. The cutoff frequency increases as the discharge current is increased, but this increase is not proportional to the square root of the current as given in Ref. 5. In order to clarify the wave phenomena, the hollow cathode was pulled from the thruster and set up in a small vacuum chamber. In this experiment, the distance between the keeper electrode and the collector was changed, the fundamental frequency of oscillation was changed, and the fundamental frequency of oscillation was measured. Table 2 shows the fundamental frequency as a function of distance. The frequency is inversely proportional to the distance, but it can not be confirmed whether the wave is an acoustic standing wave or a one way propagating wave as described in Ref. 5.

The beam current is modulated by the discharge plasma oscillations. This is shown in Figs. 12a and 12b. In Fig. 12a, the spectra at 20, 40, and 60 kHz are caused by the discharge current oscillations. The narrow-band noise at odd multiples of 10 kHz results from the power supply switching frequency. The preceding data were obtained with a thruster having a cathode keeper electrode whose aperture diameter was 1 mm (the thruster uses a closed-type hollow cathode). A coherent wave pattern was also observed in a thruster having a 2-mm orifice cathode. The spectra shifted to higher frequencies as

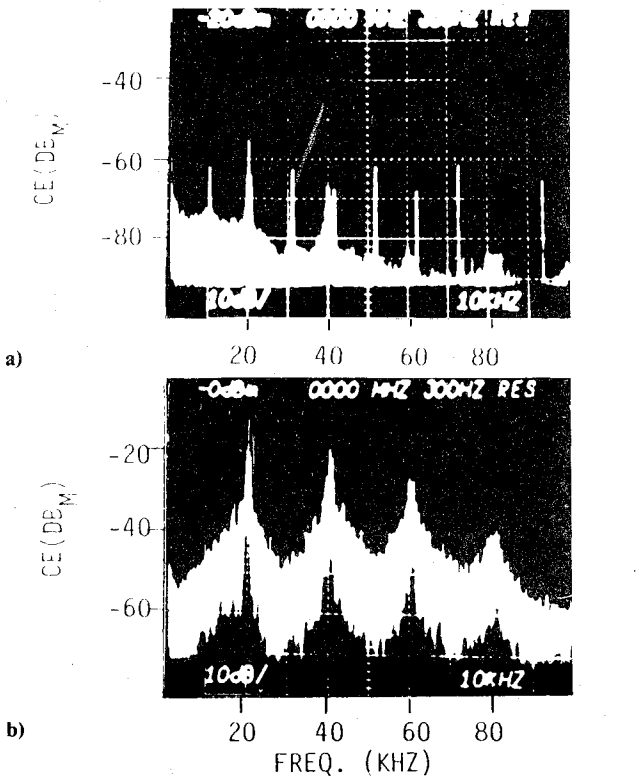


**Fig. 12 a) Beam current modulation spectra and b) discharge current spectra when a was taken.**

**Table 2 Frequency distance relationship**

| *F*, kHz | *L*, cm |
|---|---|
| 200 | 0.7 |
| 100 | 2.0 |
| 20 | 4.3 |

shown in Fig. 13. This may be the result of a higher plasma density. Though the relationship between the ion plasma wave and the ion acoustic wave has been discussed in Ref. 6, no distinction plasma wave was observed in this experiment.

The ion acoustic waves appeared at relatively low discharge voltage and low beam current, while accelerator impingement current was high. This condition is inappropriate for the ion thruster operation. At the electromagnetically silent region from 36 to 38 V discharge voltage, the ion production cost is good, but the accelerator current is still high. This is probably because the performance of the discharge chamber system and accelerating system is not well matched. That is, the thruster can be improved.

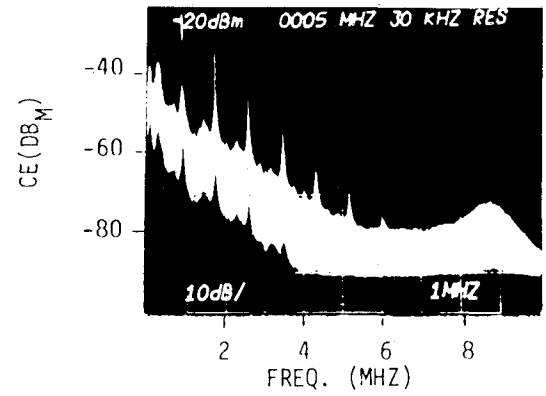


**Fig. 13 Ion wave photo for another thruster with a 2-mm main hollow orifice.**

## Conclusion

Electromagnetic noise measurements were carried out for a 5-cm diam ion engine system. Although out-of-specification points were observed when MIL-STD-461A was applied, the measured values satisfied the specification applied for the ion engine system on the ETS-III satellite. It was found that there were three discharge modes of thruster operation. Ion acoustic waves were generated spontaneously at low discharge voltages. In this mode, beam focusing was lost and the noise amplitude was 30 dB over the MIL specification. A relatively narrow discharge voltage range from 36 to 38 V was found to minimize the noise from the thruster.

## Acknowledgment

The authors express their appreciation to L.C. Pless of the Jet Propulsion Laboratory for discussions.

## References

[1]Machida, K., Toda, Y., Murakami, H., and Kudo, I., "Integration Compatibility of Ion Engine Power Conditioner," AIAA Paper 81-0691, April 1981.

[2]Toda, Y., Machida, K., Hirata, M., Murakami, H., Goseki, S., and Kudo, I., "The Thermal Vacuum Test of the Ion Engine System," AIAA Paper 81-0755, April 1981.

[3]Kudo, I., "Development of an Electron Bombardment Ion Engine," *Researches of ETL*, No. 810, Dec. 1980, p. 101.

[4]Azuma, H., Nakamura, Y., Kudo, I., Kubo, M., and Sasaki, T., "Test Chamber for Ion Engine Mounted on Satellite," AIAA Paper 81-0725, April 1981.

[5]Tanaca, H., Hirose, A., and Koganei, M., "Ion-Wave Instabilities in Mercury-Vapor Plasma," *Physical Review*, Vol. 161, Sept. 1967, pp. 94-101.

[6]Tanaca, H., Koganei, M., and Hirose, A., "Dispersion Relation of Ion Waves in Mercury-Vapor Discharges," *Physical Review Letters*, Vol. 16, June 1966, pp. 1079-1081.

[7]Amagishi, Y., "Excitation of Electron Oscillation by Ion-Acoustic Wave," *Journal of the Physical Society of Japan*, Vol. 29, Sept. 1970, pp. 764-768.